

# IRAS 17393–3004, a late-type supergiant surrounded by a dust shell

S. Philipp<sup>1</sup>, R.J. Tuffs<sup>2</sup>, P.G. Mezger<sup>1</sup>, R. Zylka<sup>3,1</sup>

<sup>1</sup> Max-Planck-Institut für Radioastronomie, Auf dem Hügel 69, D-53121 Bonn, Germany (sphilipp/rzylka@mpifr-bonn.mpg.de)

<sup>2</sup> Max-Planck-Institut für Kernphysik, Saupfercheckweg, D-69117 Heidelberg, Germany (rjt@ruby.mpi-hd.mpg.de)

<sup>3</sup> Institut für Theoretische Astrophysik, Tiergartenstraße 15, D-69121 Heidelberg, Germany (zylka@ita.uni-heidelberg.de)

Received 7 July 1999 ; accepted 21 July 1999

**Abstract.** Infrared observations of IRAS 17393–3004, including a full scan ISOSWS<sup>1</sup> are presented. The ISOSWS spectrum shows two prominent dust emission peaks at  $\lambda 10.4\mu\text{m}$  and  $17.5\mu\text{m}$  confirming that the source is a luminous star surrounded by a dust shell. The spectrum of the star, deduced from modeling of the radiative transfer through a spherical shell using the *DUSTY* code (Ivezić et al. 1997), can be explained along with other known properties in terms of an M4 supergiant with OH, SiO and H<sub>2</sub>O maser emission and a large mass loss of  $\sim 10^{-4}\text{ M}_\odot\text{ yr}^{-1}$ .

**Key words:** Stars: supergiants – late type – fundamental parameters – winds, outflows – Infrared: stars

## 1. Introduction

Although not prominent in the IRAS all sky survey due to confusion with diffuse dust emission, IRAS 17393–3004 (galactic coordinates  $l = -1^\circ 19' 57''$ ,  $b = -0^\circ 02' 38''$ ) has special interest as the brightest discrete source in the galactic plane within  $\pm 2.0$  degrees of the galactic center at infrared wavelengths shorter than ca.  $5\mu\text{m}$ . Strip scans in the range  $-2.0 \leq l \leq +2.0$  degrees, taken with the ISOPHOT instrument on ISO as part of a program to investigate the physical state and characteristics of the Nuclear Bulge (NB) (Philipp et al. 1999; Mezger et al. 1999) show the source to be brighter even than Sgr A West by a factor of 1.6 when viewed through a  $99''$  aperture in broad band filters centred on  $3.6\mu\text{m}$ .

The designation of IRAS 17393–3004 (the name we adopt for this letter) in three NIR/MIR source catalogues together with the corresponding source positions are given in Table 1. The source has been extensively observed since its discovery in the objective-prism Two-Micron Sky Survey by Hanson & Blanco (1975), who classified it as a star of *spectral type M1, peculiar with emission near 8600 Å*. IRAS 17393–3004 is seen towards the HII region Sgr E, which is believed to be located in

*Send offprint requests to:* S. Philipp, Bonn

*Correspondence to:* sphilipp@mpifr-bonn.mpg.de

<sup>1</sup> ISO is an ESA project with instruments funded by ESA Member States (especially the PI countries: France, Germany, The Netherlands and the United Kingdom) with the participation of ISAS and NASA.

**Table 1.** Designation and position of IRAS 17393–3004

Designation	$\alpha_{1950}$	$\delta_{1950}$	Ref.
IRAS 17393–3004	$17^h 39^m 22.4^s$	$-30^\circ 04' 20''$	[1]
AFGL 1977	$17^h 39^m 22.9^s$	$-30^\circ 04' 23.0''$	[2]
IRC-30316	$17^h 39^m 30^s$	$-30^\circ 04' 54.0''$	[3]

[1] IRAS Point Source Catalogue, 1985

[2] Grasdalen et al. 1983

[3] Neugebauer & Leighton 1969

the NB (Liszt 1992). It is also listed in the catalogue of OH/IR stars (te Lintel Hekkert et al. 1989) as source No. 145, where it is suggested to be a giant or an AGB star with a large mass outflow ( $\dot{M} > 10^{-5}\text{ M}_\odot\text{ yr}^{-1}$ , Olnon et al. 1981). It shows an unusually large ( $\Delta v \sim 53\text{ km s}^{-1}$ ) peak separation in the OH spectrum indicative of a massive central star; the central velocity of the OH emission determined using the separation of the two OH lines is close to zero (te Lintel Hekkert et al. 1989). IRAS 17393–3004 also shows SiO and H<sub>2</sub>O maser emission (Hall 1990; Haikala et al. 1994; Lewis et al. 1995 and Sevenster et al. 1997). These maser characteristics suggest the central star to be a supergiant. Grasdalen et al. (1983) investigated the source in the NIR/MIR broadband continuum. Volk & Cohen (1989) present an IRAS-LRS spectrum of this source showing structure at MIR wavelengths. In the IRAS data base the source is classified as having a high probability to be variable. The ISOGAL survey excluded the region around IRAS 17393–3004 (priv. comm. A. Omont). Although covered by the MSX<sup>2</sup> survey, no parameters for this source are available as yet (priv. comm. S. Price). No optical counterpart is seen on the POSS, neither has X-ray emission been found (ROSAT data archive; priv. comm. Y. Sofue for ASCA). There is a probable radio counterpart to IRAS 17393–3004, in the form of source 9 in Table 3 of Liszt (1992), which has a flux density of 21 mJy in a band of width 12.5 MHz centred at 1616 MHz, and is extended ( $15'' \times 10''$  at p.a.  $13^\circ$ ). No counterpart is seen in the National Radio Astronomy Observatory Very Large Array Sky Survey (NVSS 1995) at  $\lambda 20\text{ cm}$ . This may either indicate a

<sup>2</sup> Midcourse Space Experiment, a Ballistic Missile defense Office satellite.

**Table 2.** NIR flux density measurements of IRAS 17393–3004

	NIR Band		
	J	H	K
$\lambda/\mu\text{m}$	1.25	1.65	2.2
$S_\nu/\text{Jy}$	12.4	51	74

variable radio continuum and/or the presence of the 1612 MHz OH line in Liszt's measurement. Here we report on observations of IRAS 17393–3004 made with the SWS (de Graauw et al. 1996) and ISOPHOT (Lemke et al. 1996) instruments on board ISO, together with ground-based NIR photometry.

## 2. Observations

### 2.1. NIR and FIR Continuum observations

Coverages of a  $7' \times 5.5'$  field centred on IRAS 17393–3004 were made using the ISOPHOT-C  $3 \times 3$  pixel detector array in two spectral passbands. To avoid complete saturation of the detector the C50 (bandpass 40 - 93  $\mu\text{m}$ ) and C105 (bandpass 89 - 125  $\mu\text{m}$ ) filters were used. Since IRAS 17393–3004, although bright, is barely discernable at  $\lambda > 40 \mu\text{m}$  against the structured background emission from the galactic plane at the angular resolution of  $45''$ , the P32 mode was used to give the best available sky sampling. The data were reduced with version 7.1 of the ISOPHOT Interactive analysis package (Gabriel et al. 1997), and further corrected for the transient behaviour of the detector. An unresolved source was detected at the position of IRAS1793-3005 in the C50 filter with flux density  $37 \pm 12 \text{ Jy}$  at a reference wavelength of  $61 \mu\text{m}$  (after colour correction assuming a  $\nu^{+4}$  spectrum). A (confusion limited) upper limit of  $20 \text{ Jy}$  was obtained in the C105 filter.

In addition, the source was observed with the ESO-MPG 2.2m telescope on La Silla in June 1998 using the IRAC2B camera in the J, H, and K bands. Applying the data reduction techniques described in Philipp et al. (1999), we derived the flux densities given in Table 2.

### 2.2. Spectral observations with ISO-SWS

As a follow-up to the detection of IRAS 17393–3004 as such a prominent source in the scans in  $l$  with ISOPHOT, a full spectral scan was made on 20<sup>th</sup> February 1998 in the 2.38 - 45  $\mu\text{m}$  spectral range using the SWS instrument in AOT01 mode with scanning speed 3. The pointing was specified directly towards the probable radio counterpart measured by Liszt (1992) at (B1950)  $17^h39^m22.7^s - 30^\circ04'16.0''$ , thus ensuring that the full  $15'' \times 10''$  extent of the radio source (at p.a.  $13^\circ$ ) would be enclosed by the SWS apertures for the position angle of the observation. The spectrum was fully reduced with IA and OSIA (version of November 25<sup>th</sup> 1998 and Version 1.0 respectively; Thronley et al. 1997) starting with the latest pipeline data product (OLP V7.01). Deglitching, dark current subtraction, tail modeling, photometric checks as well as updown-corrections

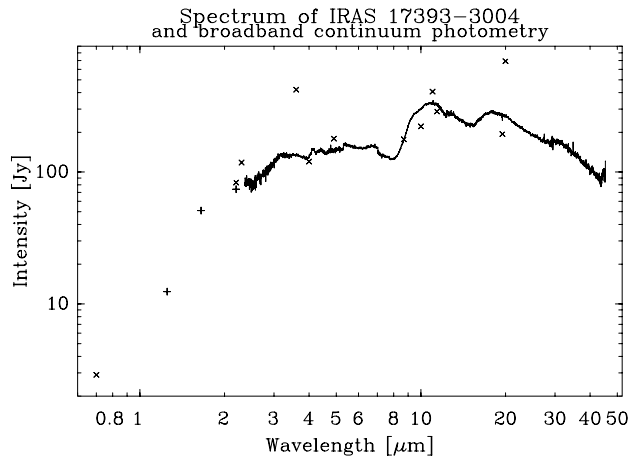


**Fig. 1.** ISOSWS spectrum of IRAS 17393–3004 and broadband continuum observations in the NIR and MIR ('x' corresponds to measurements in Grasdalen et al. (1983); '+' to our NIR photometry).

and defringing were applied. The calibration used standard tables within the IA derived from observations of Uranus; the overall uncertainty is estimated as  $\sim 30\%$  (priv.comm. SWS data centre). In Fig. 1 the ISOSWS spectrum is shown supplemented by the earlier broadband continuum observations from Grasdalen et al. (1983), and by the recent NIR observations.

The SWS spectrum shows prominent broad emission and/or absorption features due to dust and molecules, superimposed on a smooth continuum. As confirmed by the detailed modeling (Sect. 3.2) the continuum seen by SWS makes a transition from reddened photospheric-dominated emission in the NIR wavelengths to warm dust emission in the MIR. The spectral peaks at 10.4 and 17.5  $\mu\text{m}$  are most readily identified as silicate emission features. Although the shorter wavelength feature is normally centred at shorter wavelengths in the 9 - 10  $\mu\text{m}$  range, it appears here superimposed on broad-band molecular absorption from gaseous SiO, whose absorption minimum is seen around 8  $\mu\text{m}$ . SiO bandheads are seen in the range 4.0 and 4.3  $\mu\text{m}$  (this structure is discussed for cool stars in detail by Aringer et al. 1999). The other very deep molecular absorption bands in the  $\lambda$  2.5 to 9  $\mu\text{m}$  region can be ascribed to H<sub>2</sub>O. In this regime the spectrum is very similar to synthetic spectra of K and M giants and supergiants (Decin et al. 1997; Tsuji et al. 1997); comparison shows that specifically H<sub>2</sub>O is prominent in IRAS 17393–3004. Taken together, the solid-state and molecular features indicate that IRAS 17393–3004 is an oxygen-rich high mass-loss star. Although [Si II] is seen at  $\lambda$  34.8  $\mu\text{m}$ , other fine structure lines are not prominent, the feature at  $\lambda$  11.05  $\mu\text{m}$  being an artifact of the calibration (priv. comm. D. Lutz and D. Kunze).

### 2.3. Infrared Variability?

Although the IRAS variability flag was set, we were not able to confirm variability between the IRAS and ISO epochs after

a detailed comparison of the SWS spectrum and HIRES IRAS maps. Due to confusion, the source is not seen in IRAS HIRES maps in the 60 and 100  $\mu\text{m}$  bands and barely seen in the 25  $\mu\text{m}$  band. Both the flux density obtained from the 12  $\mu\text{m}$  HIRES map ( $290 \pm 30$  Jy) and the value 256 Jy derived by Haikala et al. (1994) and IRAS Point Source Catalogue (1985) and for the same band are consistent with a spectral average of the SWS data over the spectral response function of IRAS through the 12 micron band, which yields 281 Jy.

Some evidence for spectral variability is however provided by a comparison of the IRAS-LRS spectrum (Volk & Cohen 1989) and the SWS spectrum (Fig. 2). While the overall spectral distribution is similar, the line to continuum contrast of the silicate features differ between the datasets. The continuum level on the IRAS-LRS spectrum lies markedly below that of the SWS level, though it is not clear why this should be bearing in mind the consistency of the IRAS survey data with the SWS photometry and the fact that the Haikala et al. (1994) IRAS 12  $\mu\text{m}$  flux density was used to calibrate the LRS spectra, for which there were no obvious technical problems (priv. comm. R. Waters & LRS database 1987). Probably these differences might also be caused by the extraction of the spectrum from a crowded region, showing a strong gradient in the background (K. Volk, priv. comm). Inspection of Fig. 1 shows that the Grasdalen et al. (1983) flux densities in the 2 - 20  $\mu\text{m}$  spectral range, measured in the 1970's, may also support a picture of spectral variability. While most of the data points are consistent with the SWS data, the values for the pass-bands centred on  $\lambda 3.6 \mu\text{m}$  and 20  $\mu\text{m}$  are higher by more than a factor 2. One can speculate that the 20  $\mu\text{m}$  observations may be affected by atmospheric variations; the discrepancy of the 3.6  $\mu\text{m}$  observation is not really understood.

### 3. Modeling of the spectrum

#### 3.1. Nature of the star

The previous observations listed in Sect. 1 suggest that the star powering IRAS 17393–3004 is a supergiant of spectral type M. Elias et al. (1981) investigated late-type supergiants in our Galaxy and in the Magellanic Clouds, obtaining  $M_V = -8$  and  $M_K = -12$  as upper limits. The extreme case corresponding to these limits is for spectral type M4I (see e.g. Lang 1992), for which we estimate a stellar luminosity of  $\sim 1.3 \times 10^5 L_\odot$ , using the definition for absolute bolometric luminosity given by Lang (1974, Eq. (5)-(237)). Combining this luminosity with the observed K band flux density of  $S'_K = 74$  Jy (2.33 mag) yields an upper limit for the distance  $D \leq 7.335$  kpc (disregarding any extinction by dust), placing IRAS 17393–3004 in front of the NB. This is also supported by the system velocity of the maser of  $\sim -7 \text{ km s}^{-1}$  (Haikala et al. 1994), which does not coincide with the rotation curve of the NB. In fact the near-IR colours are consistent with the exciting star being close to the limiting case of an M4I supergiant. For such a star we estimate, based on the fact that IRAS 17393–3004 has no optical counterpart on the POSS, that the sum of dust extinction in the shell (expressed in terms of visual extinction)  $A_{\text{vis,shell}}$  and in the inter-

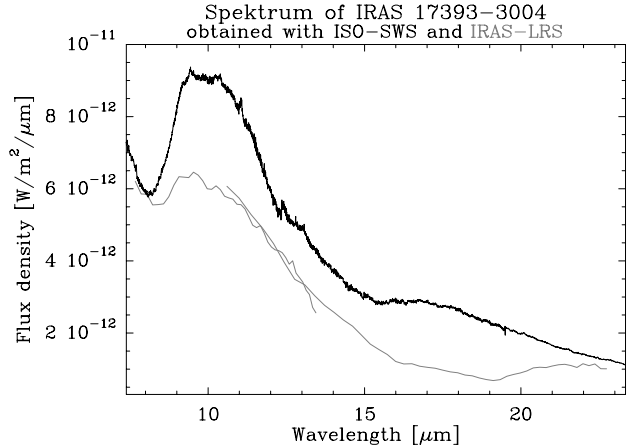


**Fig. 2.** Part of the ISOSWS spectrum of IRAS 17393–3004 (heavy curve) compared to the IRAS-LRS spectrum (dotted curve; Volk & Cohen 1989).

vening dust between the sun and the supergiant  $A_{\text{vis,ISM}}$  would be  $A_{\text{vis,shell}} + A_{\text{vis,ISM}} \geq 14$  mag. Such an extinction would place our NIR flux densities in the correct regime of colours given by Elias et al. (1985) in Table 10 for M4 I stars.

#### 3.2. Modeling the Dust Emission

The above considerations have led to a scenario for IRAS 17393–3004 in which a supergiant of spectral type M4 undergoes a strong mass outflow resulting in a shell of gas and dust surrounding the star for which we estimate a total luminosity close to  $\sim 1.3 \times 10^5 L_\odot$ . The inner radius of the dust shell  $R_{\text{in}}$  is constrained by the fact that grains are probably needed to form a sufficiently copious amount of molecules to account for the maser source. For a star with the above luminosity maser must occur within  $\sim 10^{16}$  cm for OH masering (Engels et al. 1983) and  $\leq 10^{15}$  cm for H<sub>2</sub>O masering (Elitzur 1992). The outer bound on the masering region for H<sub>2</sub>O is indeed quite close to the sublimation radius for black body grains of  $\sim 3 \times 10^{14}$  cm for this stellar luminosity and a sublimation temperature of 1230 K.

To check that the SWS spectrum of the dust emission is consistent with this scenario, and to derive parameters for the dust outflow, we have modeled the dust emission using the DUSTY code (Ivezic et al. 1997; Ivezic & Elitzur 1997 and 1995). This solves the spherical radiative transfer problem employing a scaling approach, taking the grains to be distributed from a condensation radius to at least the radius beyond which the grains become too cool to contribute to the SWS spectrum. In fact it is also possible to successfully model the dust emission spectrum in terms of a completely optically thin shell with a much larger inner boundary and an outer radius cutoff. If true this might imply some variability in the recent dust production rate. However we regard this as inconsistent with the evidence (from the H<sub>2</sub>O maser emission as discussed above) that grains are being formed at or near the condensation radius. Moreover,

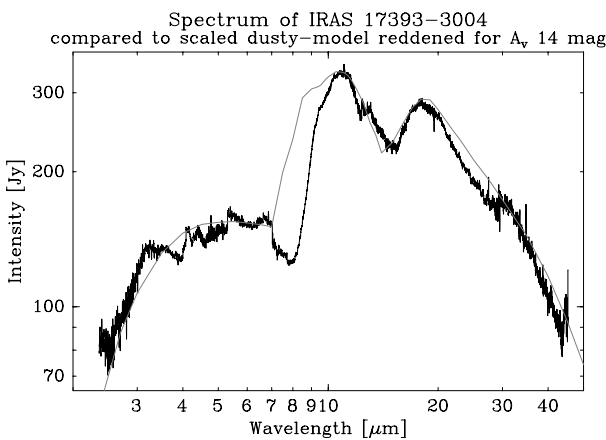


**Fig. 3.** SWS spectrum of IRAS\* 17393–3004 overlaid with the best fit *DUSTY* model (see text).

there is no completely convincing evidence for variability in the warm dust emission (see Sect. 2.3).

*DUSTY*'s output provides a self-similar set of solutions possessing scaling properties (Ivezic & Elitzur 1997). This allows a modeling in two steps. In a first step we adopt  $\tau_K \sim 1.57$  (corresponding to  $A_{\text{vis}} \sim 14$  mag) as the optical depth of the dust shell,  $T_{\text{BB}*} \sim 3000$  K as the stellar temperature and 1230 K as the condensation temperature. Subsequently, we fine tune the observed spectrum by varying the temperature of the illuminating black-body source, and the condensation temperature. Variations of  $\sim 10\%$  in these parameters are clearly noticeable in the shape of the model spectrum. No attempt is made to model the molecular and atomic absorption/emission line spectrum. For the density profile we used the analytical approach for a radiatively driven wind, available in *DUSTY* (see Ivezic et al. 1997). The chemical composition of the dust was also varied to find the best fitting model using the six common grain types contained in *DUSTY* and the standard grain size distribution from Mathis et al. (1977). The gas to dust ratio is set to 200 by *DUSTY*.

The best fit to the ISOSWS spectrum is shown in Fig. 3. It was obtained for a temperature of the embedded source of  $T_{\text{BB}*} \sim 2980$  K,  $A_{\text{vis}} \sim 14$  mag, and a dust condensation temperature of 1230 K. The dust composition was set to 60% silicates and 40% graphite grains within the model of Draine & Lee (1984). The fraction of graphite grains might be quite high for an oxygen-rich star, but such a high fraction is necessary to fit the observed flat slope at longer wavelengths. From discussions with M. Elitzur (priv. comm.) we learned, that some asymmetrical silicate grains show properties very similar to the graphite grains used here, and that this kind of grains are actually found in oxygen-rich stars. In fact such grains will be included in the subsequent version of *DUSTY*.

The largest difference between the observed and modeled spectra occurs in the range  $\lambda 7 - 10 \mu\text{m}$ . We attribute this partly to the presence of SiO absorption which is not modeled by *DUSTY*. In addition this feature may be partly due to the

presence of some uncommon silicates in the shell of IRAS 17393–3004, in which case the shape of the spectral feature would not be typical. In addition there could be a combination of emission by the dust shell and absorption by the interstellar dust. This suggestion is supported by the fact that the ISM silicate absorption peaks at a slightly shorter wavelength than the usual 9.7 micron emission peak. In addition the observed spectrum shows a weak emission feature at about  $\lambda 30 \mu\text{m}$ . This may either indicate emission from cooler dust in a detached shell, or dust emission features from crystalline Mg-rich silicates in the  $20 - 45 \mu\text{m}$  range (e.g. Henning 1999). The other smaller variations between the model fit and the observed spectrum presumably reflect possible variations of the chemical composition and/or grain size.

In a second step we scale the model by integrating the flux density of the model spectrum  $F_\lambda$  to find the bolometric luminosity, which is normalized to  $L_* \sim 1.3 \times 10^5 L_\odot$ , as estimated in Sect. 3.1. This yields a distance of the star of  $D = 4.73$  kpc if all extinction occurs in the shell, consistent with the crude estimate  $D \leq 7.335$  kpc given in Sect. 3.1. Clearly, some line of sight extinction is to be expected, which would reduce the intrinsic absorption in the shell from the value adopted in the modeling, and reduce the distance to the star. As discussed below, this is not a very sensitive parameter, especially in comparison with the condensation temperature parameter. To explore this effect we also made calculations assuming a line of sight extinction of 5 mag. This would reduce the extinction within the shell to  $\sim 9$  mag. Our computations show that this model will lead to a condensation radius which is only  $\sim 10\%$  smaller and to a mass loss rate which is only  $\sim 20\%$  lower. This leads us to consider our results to be upper limits of the actual stellar and associated parameters with an estimated uncertainty of  $\sim 30\%$ , mainly caused by the calibrational uncertainty of the ISOSWS data.

We return to our original model with all extinction due to dust in the shell surrounding the central star. In this case the condensation radius scales to  $\sim 7.8 \times 10^{14}$  cm for the silicate grains, consistent with the maximum radius of  $\sim 10^{15}$  cm for the H<sub>2</sub>O maser emission (Elitzur 1992). The derived values for the gas mass loss rate and velocity of the wind are  $\sim 1.0^{-4} M_\odot \text{ yr}^{-1}$  and  $\sim 18.7 \text{ km s}^{-1}$  respectively. The model also yields a mass of  $M_* \leq 27.3 M_\odot$  for the embedded star. All these parameters are in remarkably good agreement with the basic observational constraints discussed in Sect. 3.1, in particular the identification of the star as a type M4I supergiant.

#### 4. Summary

Combining ground- and spaceborne observations we have obtained the spectral energy distribution for the IR/OH star IRAS 17393–3004 in the wavelength range  $1.25 \leq \lambda/\mu\text{m} \leq 60$ . The near-IR spectrum has JHK colours corresponding to an M4 star reddened by dust with  $A_{\text{vis}} \sim 14$  mag. The MIR spectrum shows prominent silicate peaks at  $10.4$  and  $17.5 \mu\text{m}$  as well as an SiO absorption around  $8 \mu\text{m}$  and SiO bandheads in the  $4.0 - 4.3 \mu\text{m}$  range. Taken together, the solid-state and molec-

ular features confirm the picture already suggested from the SiO, OH and H<sub>2</sub>O maser activity that IRAS 17393–3004 is a luminous oxygen-rich star with a high mass-loss dusty wind. Neglecting line of sight extinction, the broad band spectral energy distribution of the dust emission and the extinction in the near-IR can be fitted by a spherically symmetrical outflow of a silicate and graphite grain mixture illuminated by an M4I supergiant situated at a distance of  $\leq 4.73$  kpc with luminosity  $\sim 1.3 \times 10^5 L_{\odot}$ , dust production rate  $5 \times 10^{-7} M_{\odot} \text{ yr}^{-1}$  and wind velocity  $\sim 18.7 \text{ km s}^{-1}$ . For a distance of 4.73 kpc, the shell's inner boundary diameter corresponds to an angular size of  $\sim 0.022''$ , which will make it accessible in future to quantitative observations with the VLA (maser emission) and VLTI (MIR dust emission) respectively.

*Acknowledgements.* We gratefully acknowledge the support provided by the ISO data centres at MPIA in Heidelberg and MPE in Garching. We benefited much from discussions with M. Elitzur, H.-P. Gail, Th. Henning, H.-U. Käufel, D. Kunze, D. Lutz, K.M. Menten, R. Waters and A.A. Zijlstra. Our special thanks go to the referee K. Volk for his comments, from which the paper profited much.

## References

Aringer B., Höfner S., Wiedemann G. et al., 1999, A&A 342, 799

Decin L., Cohen M., Erikson K. et al., 1997, ESA-SP 419, 185

Draine B.T., Lee H.M., 1984, ApJ 285, 89

Elias J.H., Frogel J.A., Humphreys R.M., Persson S.E., 1981, ApJ 249, L55

Elias J.H., Frogel J.A., Humphreys R.M., 1985, ApJS 57, 91

Elitzur, 1992, Ap&SS Library 170, “Astronomical Maser”, 225

Engels D., Kreysa E., Schultz G.V., Sherwood W.A., 1983, A&A 124, 123

Haikala L.K., Nyman L.-A., Forstroem V., 1994, A&AS 103, 107

Hall P.J., Wright A.E., Troup E.R., Wark R.M., Allen D.A. 1990, MNRAS 247, 549

Hanson O.L., Blanco V.M., 1975, AJ 80, 1011

Henning Th., 1999, IAU Symp. 191, in press

de Graauw T., Haser L.N., Beintema D.A. et al., 1996, A&A 315, L49

Grasdalen G.L., Gherz R.D., Hackwell J.A., Castelaz M., Gullixson C., 1983, ApJS 53, 413

Gabriel, C., Acosta-Pulido J., Heinrichsen I., Morris H., Tai W.-M., 1997, PASPC 125, 108

IRAS Point Source Catalogue, 1985, US Government Publication Office

Ivezic Ž., Elitzur M., 1995, ApJ 445, 415

Ivezic Ž., Elitzur M., 1997, MNRAS 287, 799

Ivezic Ž., Nebkova M., Elitzur M., 1997, User Manual for *DUSTY*, <http://www.pa.uky.edu/~moshe/dusty>

Lang K.R., 1974, Astrophysical Formulae, Chapter 5.5

Lang K.R., 1992, Astrophysical Data: Planets and Stars, 132ff.

Lemke D., Klaas U., Abolins J., et al., 1996, A&A 315, L64

Lewis B.M., David P., Le Squeren A.M., 1995, A&AS 111, 237

te Lintel Hekkert P., Versteege-Hensel H.A., Habing H.J., Wiertz M., 1989, A&AS 78, 399

Liszt H.S., 1992, ApJS 82, 495

LRS database (IRAS Low Resolution Spectra, IRAS team), 1987, NASA RP-1190, online via <http://cdsweb.u-strasbg.fr/>

Mathis J.S., Rumpl W., Nordsieck K.H., 1977, ApJ 422, 164

Mezger P.G., Zylka R., Philipp S., Launhardt R., 1999, A&A 348, 457

NVSS Survey, 1995, data archive online via <http://oldzia.aoc.nrao.edu/doc/vladb/VLADB.html>

Neugebauer G., Leighton R.B., 1969, Two-Micron Sky Survey (NASA SP-3047), Washington, D.C.

Oloni F.M., Walterbos R.A.M., Habing H.J., Mathews H.F., 1981, ApJ 245, L103

Philipp S., Zylka R., Mezger P.G. et al., 1999, A&A 348, 768

Sevenster M.N., Chapman J.M., Habing H.J., Killeen N.E.B., Lindqvist M., 1997, A&AS 122, 79

Thronley M., Sturm E., Kunze D., Lutz D., 1997, IA User Manual, via <http://www.mpe-garching.mpg.de/iso/observer/isap/isap.html>

Tsuji T., Ohnaka K., Aoki W., Yamamura I., 1997, A&A 320, L1

Volk K., Cohen M., 1989, AJ 98, 931